X-ray and dielectric study of the phase transition in PbFe ½ Nb ½ O3 - PbCo ½ W ½ O3 ceramics

Yung Park*, Hong Min Lee**, Ho-Gi Kim*
*Department of Materials Science and Engineering, Korea Advanced Institute of Science and Technology, Kusong-dong, Yusong-gu, Taejon 305-701, Korea
** *Department of Electronic Engineering*
Kyonggi University, Suwon, Kyonggi Do, Korea

Abstract.
A phase analysis in the solid solution of (1- χ) PbFe ½ Nb ½ O3 - χ PbCo ½ W ½ O3 is conducted by dielectric properties, heat capacity and *E-P* hysteresis at χ =0.1 interval. Lattice constants and superlattice intensity are analyzed by the x-ray diffraction, and the temperature - composition phase diagram is determined. The system is found to form a solid solution of perovskite structure throughout the entire composition range, but the nature of phase transitions changes from ferroelectric-paraelectric for $0 \le \chi \le 0.5$ to antiferroelectric-paraelectric for $0.6 \le \chi \le 1.0$. The transitions of ferroelectric-paraelectric and antiferroelectric-paraelectric for $0.2 \le \chi \le 0.5$ and for $0.6 \le \chi \le 0.8$, respectively, are diffuse, while those of the ferroelectric-paraelectric and the antiferroelectric-paraelectric for $0.0 \le \chi \le 0.1$ and $0.9 \le \chi \le 1.0$, respectively are sharp.

1. Introduction
It is well known that two isostructural ferroelectrics can form a solid solution. A number of perovskite solid solutions such as (Ba,Sr)TiO3 [1] and lead lanthanum zirconium titanate (PLZT) [2] show peculiar phase transition behaviors in certain composition ranges. This type of phase transition is named diffuse-phase transition (hereafter abbreviated as DPT), and DPT phenomena have been summarized as followings: i) broadened maxima in the dielectric constant curves and ii) different transition temperatures by different physical parameters [3].

One measure of the extent of the DPT is given by the broadness of the dielectric constant against temperature curves. The best fit to the curve for the DPT dielectric constant near the phase transition has been presented in the form [4,5]

$(Km - K)/K = (Ta/\sigma)^n (T/Ta - 1)^n$

where Km is the maximum value of the dielectric constant at the apparent transition temperature Ta, σ is a measure of the extent of thermal diffuseness, and n is an exponent also of another measure of the DPT. In extreme case of $n = 1$, σ is simply a Curie-Weiss constant, while σ^2 approximates a degree of the temperature fluctuation of the polarization distribution in a Gaussian approximation for $n = 2$ [4]. The exponent of n can be determined from the slope of the log-log plot of above equation while σ can be determined from y-axis intercept of the same plot. Both n and σ can together indicate the extent of the DPT.

It has been found in this study that ferroelectric PbFe ½ Nb ½ O3 and antiferroelectric PbCo ½ W ½ O3 form a solid solution in the entire composition range, and the PbFe ½ Nb ½ O3 - PbCo ½ W ½ O3 solid solution undergoes diffuse ferroelectric-paraelectric and antiferroelectric-paraelectric phase transitions in the intermediate composition range. In that PbFe ½ Nb ½ O3 is disordered, while PbCo ½ W ½ O3 is ordered, the phase transitions of this solid solution are interesting. Hereinafter, for convenience, PFN and PCW will be used to denote PbFe ½ Nb ½ O3 and PbCo ½ W ½ O3, respectively.

At room temperature, the PFN composition is ferroelectric with perovskite-type crystal structure, in which Fe^{+3} and Nb^{+5} ions are randomly distributed in the octahedral positions. The phase transition occurs at 112 ℃ [6] from rhombohedral (ferroelectric) to cubic (paraelectric).

On the other hand, the PCW perovskite composition has a highly ordered *B*-site sublattice. There has been much debate in the literature concerning the nature of the ferroelectric phase below the transition at 32 ℃, be it an antiferroelectric [7,8] or ferroelectric displacive phase transition [9,10]. Another study of the transition temperatures as a function of hydrostatic pressure strongly suggests that the PCW has an antiferroelectric nature below *Tc* . Brixel *et al.* [9], Tamura [10], and Filip'ev and Fesenko [11] all have suggested the symmetry to be monoclinic. Tamura, in an x-ray study, noted the existence of an incommensurate phase in PCW down to -123 ℃.

The scope of this study is to investigate the various physical properties of pseudobinary PFN-PCW ceramics as a function of temperature and composition: lattice constants, dielectric properties, heat capacity and *E-P* hysteresis loop. The temperature-composition phase diagram of PFN-PCW ceramics is determined. The apparent phase transition could be determined from the peak of the heat capacity curve.

2. Experiment
All the specimens were synthesized by the conventional ceramic process. The starting materials were powders of PbO (purity 99.5%), Fe2O3 (99.5%), Nb2O5 (99.5%), CoO (99.5%) and WO3 (99.9%). The raw materials weighed in appropriate proportions for (1- χ) PbFe ½ Nb ½ O3 - χ PbCo ½ W ½ O3 formula with χ at 0.1 interval were wet-ball milled for 24 h, dried, and then calcined at 850 ℃ for 2 h. The calcined powders were ground again by wet-ball milling and then pressed into disk shape. The green compact was sintered at 900 ~ 1050 ℃ for 2 h and electroded with silver paste.

Sintered ceramics were crushed to an average particle size of 40 μm to achieve an optimal orientation for x-ray diffraction analysis. Powder x-ray diffractions were conducted using an x-ray diffractometer in order to calculate the lattice constant by using a commercialized least-square determination. The dielectric constant was measured with LCR (Hewlett Packard 4294A) at 1 kHz, 10kHz, 100kHz and 1000kHz. The heating rate was maintained at 5 ℃/h during dielectric property measurements. The dielectric phase state was analyzed by *E-P* hysteresis loop obtained by a modified Sawyer-Tower circuit [11]. The frequency of the applied field was 60 Hz, and *E-P* hysteresis loop was observed on an oscilloscope (Hewlett-Packard 54601B) in the temperature range of -100 ℃ to 120 ℃. Heat capacities of specimens with differing χ concentrations were obtained in the temperature range around the phase transition temperature using Stanton DSC differential scanning calorimetry. The heating rate was maintained at 5 ℃/h.

3. Results

3.1. x-ray diffractions
Room temperature x-ray diffraction patterns for powders of pseudobinary (1- χ) PFN - χ PCW ceramics show that a perfect solid solution is formed in the entire composition range. The unit cell parameters - lattice constant and β - of the solid solution as a function of χ at room temperature are illustrated in figure 1(a).

According to Smolenskii and Bokov [14], the crystal structure of PFN at room temperature is rhombohedral (slightly distorted from cubic structure). In this study the crystal structure is nearly rhombohedral at room temperature.

For $0.0 < \chi < 0.2$, the solid solution also appears to be rhombohedral at room temperature, while, for $0.2 \le \chi \le 0.9$, the solid solution is cubic, and lattice constant appears to vary continuously as a function of χ. Finally, the structure of pure PCW is observed to be monoclinic.

X-ray diffraction patterns reveal three superlattice reflections about (h+½,0,0), (h+½,k+½,0) and (h+3/2,k+½,0) which correspond

to the ordering of Co^{+2} and W^{+6} cations on the perovskite B site sublattice. Figure 1 (b) illustrates that superlattice reflection intensity of (h+½,k+½,0) increases with increasing χ.

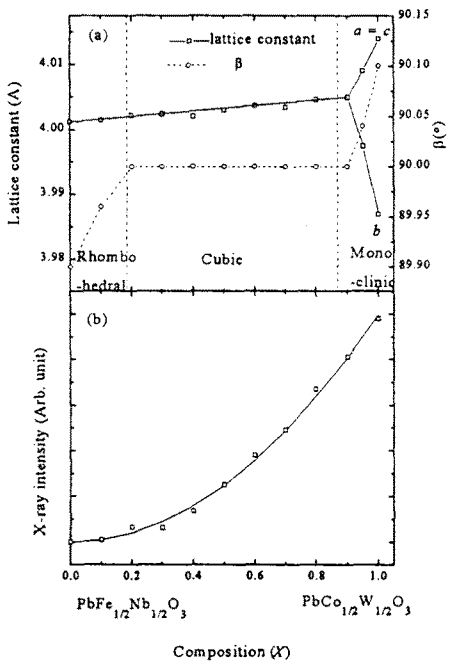

Figure 1 (a) Changes in unit cell constants of solid solution in (1-χ)PbFe ½ Nb ½ O3 -χ PbCo ½ W ½ O3 ceramics at room temperature, and (b) integrated intensity of superlattice reflection (h+½,k+½,0) at room temperature.

3.2. Dielectric properties

The variations of the relative dielectric constant as a function of temperature at different compositions are shown in figure 2. The absolute values of dielectric constant decrease with increasing χ. The temperature *Ta* of the dielectric constant maximum decreases with increasing χ until it reaches a minimum at $\chi = 0.7$ and then increases with increasing χ for $0.7 \le \chi \le 1.0$. The temperature *Tb* of the dissipation factor maximum behaves similarly as *Ta* and its minimum value occurs also at $\chi = 0.7$. The characteristic behaviors of the dielectric constant and of the dielectric dissipation factor in three different composition ranges are summarized in the followings:

i) $0.0 \le \chi \le 0.1$ The dielectric constant curves have relatively sharp maxima and there absolute values are large. For $\chi = 0.0$, the frequency dependence of dielectric constant and dielectric dissipation factor as a function of temperature is also relatively small, as can be seen in figure 3(a). There is discrepancy between *Ta* and *Tb*. *Ta* is higher than *Tb*. $\delta T\square$ is defined as the difference between *Ta* and *Tb*, $\square$ is the measured frequency. Figure 4 shows that the exponent *n* and the difference between the two temperatures, $\Delta T = \delta T1000kHz - \delta T1kHz$, both of which indicate the degree of the DPT, stays close to 1.1 and 2 ℃, respectively.

ii) $0.2 \le \chi \le 0.8$ The dielectric constant curves exhibit the broadened maxima. ΔT and *n* as a function of χ are shown in figure 4. ΔT and *n* increase with increasing χ for $0.2 \le \chi \le 0.5$, reach the maximum values of 30 ℃ and 1.84, respectively, at $\chi = 0.5$, and then decrease with increasing χ for $0.5 \le \chi \le 0.8$. There is discrepancy between *Ta* and *Tb*, and they are both frequency dependent. The frequency dependence of the dielectric constant and dielectric dissipation factor as a function of temperature for $\chi = 0.5$ in figure 3(b) shows a typical characteristic of DPT material or relaxor. The dielectric constant curve shifts downward as χ increases.

iii) $0.9 \le \chi \le 1.0$ The absolute value of the dielectric constant curves are relatively small. *Ta*, *Tb* and ΔT are frequency independent and ΔT takes the value of zero. Furthermore, the frequency dependence of the dielectric response is not observed for $\chi = 1.0$ in figure 3(c).

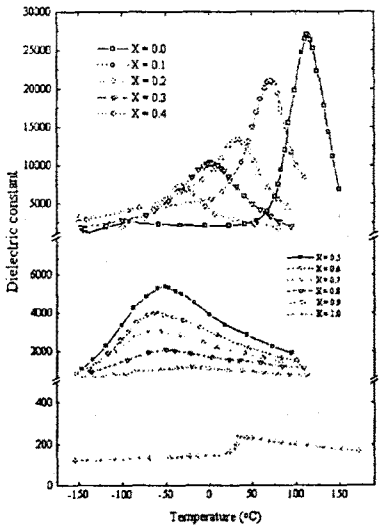

Figure 2 Dielectric constant curves of (1-χ)PbFe ½ Nb ½ O3 -χ PbCo ½ W ½ O3 ceramics at 1kHz.

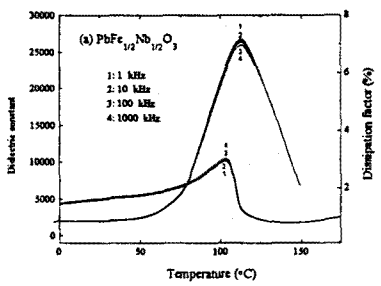

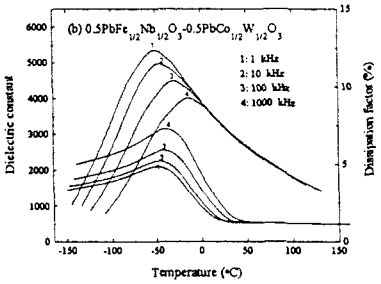

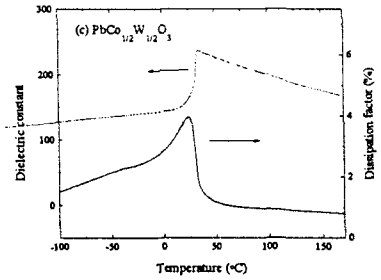

Figure 3 Temperature dependence of the dielectric constant and dissipation factor at different frequencies for (a) PbFe ½ Nb ½ O3, (b) 0.5PbFe ½ Nb ½ O3 -0.5PbCo ½ W ½ O3 and (c) PbCo ½ W ½ O3 ceramics. Figure 3(c) doesn't reveal the frequency dependence of the dielectric response.

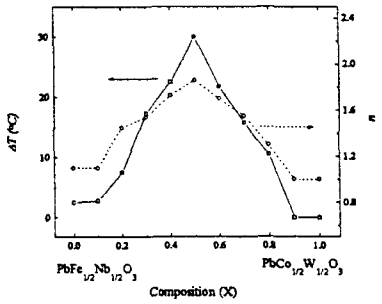

Figure 4 ΔT and n vs composition χ for (1- χ)PbFe ½ Nb ½ O3 - χ PbCo ½ W ½ O3 ceramics. *Ta* and *Tb* correspond to the dielectric constant maximum temperature and dielectric dissipation factor maximum temperature, respectively. $\delta T\square$ is defined as the difference between *Ta* and *Tb*, $\square$ is the measured frequency. The difference between the two temperatures, ΔT = $\delta T1000kHz$ - $\delta T1kHz$ and n indicate the degree of DPT.

3.3. *E-P* hysteresis loops

E-P hysteresis loops are shown in figures 5 (a)-(g). A hysteresis loop at 100 ℃ for pure PbFe ½ Nb ½ O3 shows that the low temperature phase is observed to be ferroelectric because normal ferroelectric hysteresis loop is retained up to 110 ℃ as can be seen in figure 5 (a).

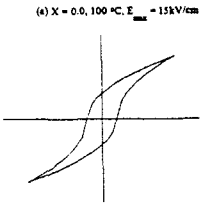

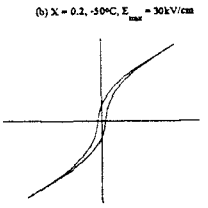

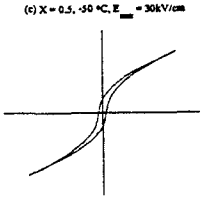

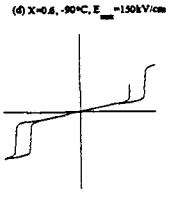

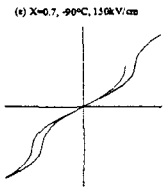

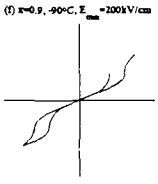

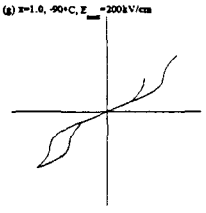

Figure 5 *E-P* hysteresis curves of (1- χ)PbFe ½ Nb ½ O3 - χ PbCo ½ W ½ O3 ceramics.

3.4. Heat capacity

Figure 6(a) shows the temperature dependence of the heat acpacity of pure PCW which was measured on heating. A sharp decrease of the heat capacity just above 32 ℃ is observed. This fact is consistent with the dielectric constant (figure 2) and further confirms that the antiferroelectric-paraelectric phase transition is of first-order. For $0 \leq \chi \leq 0.5$, the heat capacity anomaly in figures 6 (a) to (c) becomes broadened with increasing χ concentration, while , for $0.5 < \chi < 1.0$, that becomes sharp, as shown in figures 6 (c) - (e). The broad heat capacity feature of (1-χ) PFN - χ PCW is associated with the dielectric DPT.

On the other hand, figure 6 (e) shows the relatively sharp peak of heat capacity of pure PFN. It is ascribed to the B site disordering that PFN reveals the less sharp peak than PCW.

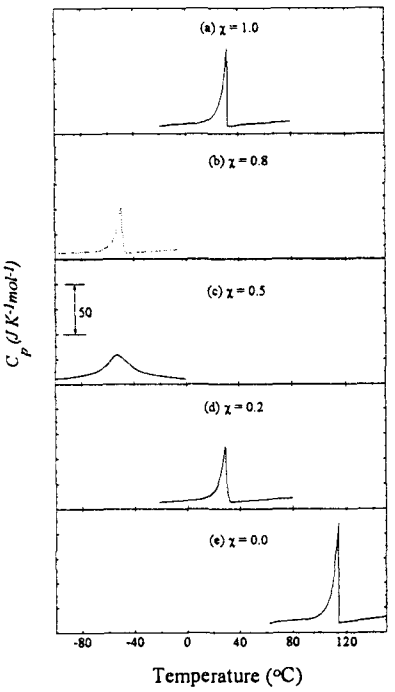

Figure 6 Variation of the heat capacity of the (1- χ)PbFe ½ Nb ½ O3 - χ PbCo ½ W ½ O3 ceramics with different χ concentrations.

4. Discussion

The x-ray diffraction patterns for (1- χ) PFN - χ PCW system show that a perfect solid solution of a single phase is formed for the entire composition range at room temperature. Based on *E-P* hysteresis loops, n and ΔT, the solid solution, as can be seen in figure 7, exhibits four different phase transitions: i) the ferroelectric phase of sharp transition, ii) the ferroelectric phase of diffuse transition, iii) the antiferroelectric phase of diffuse transition, and iv) the antiferroelectric phase of sharp transition.

Firstly, the ferroelectric phase of sharp transition was observed on $0.0 \leq \chi \leq 0.1$. In this composition range, the solid solution behaves somewhat like PbFe ½ Nb ½ O3 , and display a relatively sharp transition and a normal hysteresis loop in the ferroelectric state. ΔT is nearly frequency independent.

Secondly, the solid solution for $0.2 \leq \chi \leq 0.5$ shows the ferroelectric phase of diffuse transition. The dielectric constant curve near the maximum is broadened, and its broadness increases with increasing χ. Characteristic temperatures of Ta and Tb and ΔT are frequency dependent.

Thirdly, the antiferroelectric phase of diffuse transition appears for $0.6 \leq \chi \leq 0.8$. The shape of the dielectric constant curves in this range is similar but broader than those in the composition $0.2 \leq \chi \leq 0.5$, but its magnitude becomes smaller. The antiferroelectric double hysteresis loop of low temperature phase indicates that the solid solution in this composition ranges is antiferroelectric.

Fourthly, the solid solution for $0.9 \leq \chi \leq 1.0$ reveals the antiferroelectric phase of sharp transition. The dielectric properties of the solid solution in this composition range are similar to those of pure PCW. The phase transition occurs sharply; and its Ta, Tb and ΔT are frequency independent. The typical antiferroelectric double hysteresis loop is

observed for the low temperature phase.

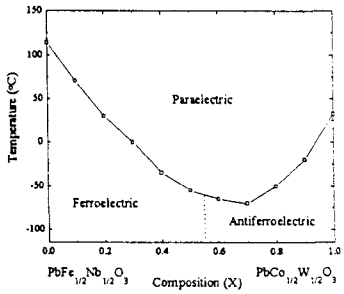

Figure 7 Dielectric phase diagram of (1- χ)PbFe ½ Nb ½ O3 - χ PbCo ½ W ½ O3 ceramics. The dashed line shows the ferroelectric - antiferroelectric phase boundary.

5. conclusions

A phase diagram of (1- χ) PFN - χ PCW solid solution has the following characteristics: at the ferroelectric end of the composition for $0.0 \leq \chi \leq 0.1$, a relatively sharp ferroelectric-paraelectric phase transition is observed; at the antiferroelectric end of the composition for $0.9 \leq \chi \leq 1.0$, a displacive antiferroelectric-paraelectric transition; in the lower intermediate composition range for $0.2 \leq \chi \leq 0.5$, a diffuse ferroelectric-paraelectric transition; in the higher intermediate composition range for $0.6 \leq \chi \leq 0.8$, a diffuse antiferroelectric-paraelectric transition. In the composition range of diffuse transition, *Ta*, *Tb*, ΔT and *n* are frequency dependent and its magnitude of ΔT and *n* take a maximum value χ = 0.5. In the sharp transition ranges the difference, ΔT, is frequency independent.

References

[1] Benguigui L and Bethe K 1969 *J. Appl. Phys.* **47** 2787
[2] Takahashi M 1971 *Jpn. J. Appl. Phys.* **10** 643
[3] Stenger C G F and Burggraaf 1980 *J. Phys. Chem. Solids* **41** 17
[4] Uchino K and Nomura S 1982 *Ferroelectrics* **44** 55.
[5] Diamond H 1961 *J. Appl. Phys.* **32** 909.
[6] Smolenski G A, Agranovskaya A I, Popov S N and Isupov V A 1958 *Zh. Tekh. Fiz.* sov. *Phys. Tech. Phys.*] **28** 2152
[7] Bokov V A, Kizhaev S A, Myl'nikova I E and Tutov A G 1964 *Fiz. Tverd. Tela* (Leningrad) **6** 3038 [1965 *Sov. Phys. Solid State* **6** 2419].
[8] Hachiga T, Fujimoto S and Yasuda N 1985 *Jpn. J. Appl. Phys . Suppl.* **24** 239
[9] Brixel W, Werk M L, Fischer P, Buhrer W, Rivera J P, Tissot P and Schmid H 1985 *Jpn. J. Appl. Phys. Suppl.* **24** 242
[10] Maaroufi F, Toledano P, Schmid H, Brixel W and Buhrer W 1988 *Ferroelectrics* **79** 295
[11] Tamura H 1978 *Ferroelectrics* **21** 449
[12] Filip'ev V S and Fesenko E G 1964 *Kristallografiya* **9** 293 [1964 *Sov. Phys. -Crystallog.* **9** 231]
[11] Diamant H, Drench K and Pepinsky R 1957 *Rev. Sci. Instrum.* **28** 30
[12] Smolenskii G A and Bokov V A 1964 *J. Appl. Phys.* **35** 915